

# Enantioselective Hydrogenations of Arylalkenes Mediated by [Ir(cod)(JM-Phos)]<sup>+</sup> Complexes

Duen-Ren Hou,<sup>[a]</sup> Joseph Reibenspies,<sup>[a]</sup> Thomas J. Colacot,<sup>[b]</sup> and Kevin Burgess\*<sup>[a]</sup>

**Abstract:** Phosphine oxazoline ligands **1a–j** were converted to the corresponding [Ir(cod)(phosphine oxazoline)]<sup>+</sup> complexes **2a–j**. X-ray diffraction analyses of complexes **2b**, **2h**, **2i**, and **2j** were performed. The *tert*-butyl-, 1,1-diphenylethyl-, and phenyl-oxazoline complexes (**2b**, **2h**, and **2i**, respectively) had typical square planar metal environments with chair-like metallocyclic rings. However, the 3,5-di-*tert*-butylphenyl oxazoline complex **2j** was distorted toward a tetrahedral metal geometry. This library of complexes was tested in asymmetric hydrogenations of several arylal-

kenes. High enantioselectivities and conversions were observed for some substrates. A possible special role for the HPh<sub>2</sub>C-oxazoline substituent in asymmetric hydrogenations was identified and is discussed. In attempts to rationalize why high enantioselectivities were not observed for some alkenes, a series of deuterium labeling experiments

were performed to probe for competing reactions that occurred prior to the hydrogenation step. Double bond migrations were inferred for several substrates, and this is a significant complication in asymmetric hydrogenations of arylalkenes that had not been discussed prior to this study. A mechanistic rationale is proposed involving competing double bond migration for some but not all substrates. Appreciation of this complication will be valuable in further studies aimed at optimization of enantioselection in asymmetric hydrogenations of unfunctionalized alkenes.

**Keywords:** alkenes • asymmetric catalysis • homogeneous catalysis • hydrogenation • N ligands • P ligands

## Introduction

Development of effective asymmetric hydrogenation reactions of unfunctionalized alkenes has been slow relative to some other reactions catalyzed by organometallic complexes. This is partly due to analytical difficulties. Alkanes do not have functional groups which interact strongly with chiral supports so their optical purities tend to be difficult to ascertain via chromatographic methods. Probably more significant is the fact that, for unfunctionalized alkenes, there is little else but steric forces available to be manipulated to achieve enantioface differentiation since polarity and hydrogen bonding effects are unlikely to be significant.

The first encouraging data reported for asymmetric hydrogenations of unfunctionalized alkenes featured cyclopentadienyl complexes of titanium and zirconium. Titanocene dichloride complexes prepared from camphor-derived, chiral cyclopentadienyl ligands were used as catalyst precursors for hydrogenation of 2-phenylbut-1-ene and 2-ethyl-1-hexene. The best optical purity was 34%, only 10 turnovers occurred. In order to obtain these data the reaction was run at –75 °C.<sup>[1, 2]</sup> Moreover, the enantiomeric excess (*ee*) values were determined by polarimetry and the intrinsic experimental error for that method is high. Similarly, others have since used zirconium catalysts functionalized by the Brintzinger bis(tetrahydroindenyl) system<sup>[3]</sup> and reported *ee* values of up to 65% based on optical rotations.<sup>[4, 5]</sup> Enantiomers of many alkanes with aromatic substituents are now resolvable on modern chiral HPLC columns, and, more recently, this technique was used to analyze hydrogenation reactions mediated by Brintzinger's titanocene catalysts. Buchwald and co-workers examined nine substrates in this way. Eight of the nine *ee* values reported were in the 83–99% range.<sup>[6]</sup> All these substrates were trisubstituted alkenes. The catalyst loading required, 2–5 mol%, was higher than ideal. Similar zirconocene catalysts were used for hydrogenations of tetrasubstituted alkenes, but the results were more variable.<sup>[7]</sup> Pinene-derived cyclopentadienyl ligands have also been

[a] Prof. K. Burgess, Dr. D.-R. Hou, Dr. J. Reibenspies  
Department of Chemistry, Texas A & M University  
P.O. Box 30012, College Station, TX 77842 (USA)  
Fax: (979)845-8839  
E-mail: burgess@tamu.edu

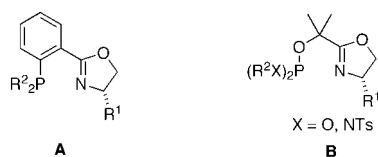
[b] Dr. T. J. Colacot  
Johnson Matthey, Catalysts and Chemicals Division  
2001 Nolte Drive, West Deptford, NJ 08066-1742 (USA)

Supporting information for this article is available on the WWW under <http://www.wiley-vch.de/home/chemistry/> or from the author: Tabulated details of the screens performed using different complexes in Reactions (2)–(6). Crystallographic data for the X-ray structural analyses are available from the author.

transformed into titanocene and zirconocene complexes and tested as hydrogenation catalysts, but the data reported was less encouraging; *ee* values of up to 69% (measured by polarimetry) were reported for two 1,1-disubstituted alkenes.

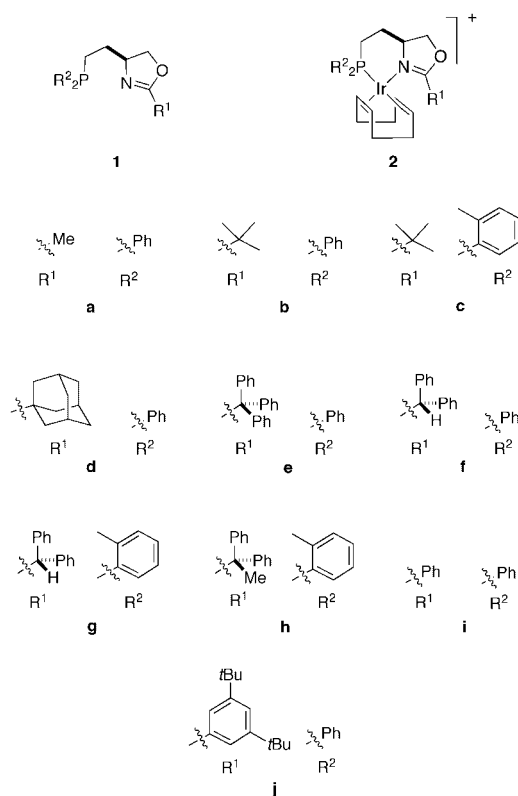
Crabtree's catalyst,  $[\text{Ir}(\text{cod})(\text{py})\text{PCy}_3]^+ \text{PF}_6^-$ , has some unique properties with respect to hydrogenation of alkenes.<sup>[8]</sup> Mechanistic studies<sup>[9]</sup> indicate that oxidative addition of hydrogen to this complex takes place with a *trans*-orientation relative to the pyridine ligand.<sup>[10]</sup> Solvent or alkene then coordinates and the COD ligand is removed by hydrogenation. Coordination of *two* alkene units to the iridium, then transformation of the resulting  $[\text{IrH}_2(\text{py})(\text{PCy}_3)(\text{alkene})_2]^+$  into hydrogenation products is apparently a prevalent pathway for many alkene substrates.<sup>[11]</sup> Relief of unfavorable steric interactions may drive the hydrogenation step, and this accounts for the fact that Crabtree's catalyst hydrogenates tri- and tetrasubstituted alkenes which are not converted by closely related rhodium complexes.

Pfaltz and co-workers prepared complexes of the type  $[\text{Ir}(\text{cod})(\mathbf{A})]^+$  ( $\mathbf{A}$  = the phosphine oxazoline shown below) and, recognizing their similarity to  $[\text{Ir}(\text{cod})(\text{py})\text{PCy}_3]^+$ , investigated these as catalysts in hydrogenation reactions of trisubstituted alkenes.<sup>[12–14]</sup> Later, they also investigated reactions of the corresponding complexes prepared from the phosphite/diazaphospholidine oxazolines  $\mathbf{B}$ . The enantioselectivities they obtained were comparable to the best results using Brintzinger's titanocene catalysts, but the conversions were higher and less catalyst was required (0.1–1.0 mol% versus  $\approx 5$  mol%).



We recently reported syntheses of the phosphine oxazoline ligands  $\mathbf{1}$ , and commented on them in relation to ligands  $\mathbf{A}$ .<sup>[15, 16]</sup> They have a curved shape, and they tend to form complexes wherein the R-functionality projects to an orientation nearer the metal than the corresponding substituent in ligands  $\mathbf{A}$ . Moreover, there is more scope for varying the R substituent in the phosphine oxazoline ligands  $\mathbf{1}$  with respect to electronic and topographical diversity. None of these considerations mean that ligands  $\mathbf{1}$  must be superior to the structures  $\mathbf{A}$ , but they do imply that complexes of these should be sufficiently different to make the comparison interesting.

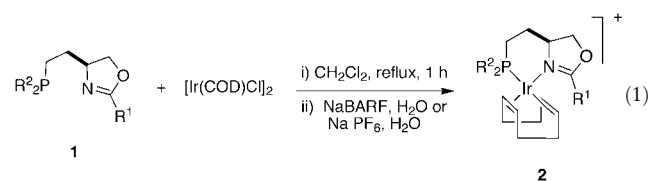
This paper describes experiments which were designed to compare ligands  $\mathbf{A}$  and  $\mathbf{1}$  in asymmetric hydrogenations of arylalkenes. The motivation for these studies was to find superior ligands for asymmetric hydrogenations of aryl alkenes. Implicit in this approach is the assumption that optimization of enantioselectivities in this process is only a function of ligand design and appropriate modification of conditions. In fact, data that emerged from these studies indicates that line of reasoning is too superficial. Specifically, deuterium labeling experiments demonstrated diminished enantioselectivities for some substrates can be attributed to



factors which are difficult to control by simple modifications of reaction conditions and/or ligand structure. The conclusions are a concern for all analogues of Crabtree's catalyst: Pfaltz's, ours and others that may be contemplated. Consequently, while the yields and enantioselectivities reported here are comparable but not superior to those reported earlier by Pfaltz, these studies lay foundations for further advances in the area by delineating obstacles which must be overcome to attain highly enantioselective hydrogenations of unfunctionalized alkenes.

## Results and Discussion

**The catalyst library:** The catalysts required for this work were prepared by Reaction (1). These materials were isolated as orange-yellow solids by crystallization, and they are not particularly air-sensitive.



Structural variance in the catalyst library as a function of the different R groups was probed by single crystal X-ray studies of compounds  $\mathbf{2b}$ ,  $\mathbf{2h}$ ,  $\mathbf{2i}$ , and  $\mathbf{2j}$  (Figure 1). The structures of the *tert*-butyl ( $\mathbf{2b}$ ), 1,1-diphenylethyl ( $\mathbf{2h}$ ), and phenyl ( $\mathbf{2i}$ ) complexes are very similar. They have typical square-planar structures in which the metalocyclic ring adopts a chair-like

conformation. Complex **2h** was the only di(2-methylphenyl)-phosphino derivative examined (the rest were Ph<sub>2</sub>P ligands) but this appeared to make no significant difference to the structure: They all crystallized with an edge-on pseudo-axial P-aryl group, while they each had a less encumbered, pseudo-equatorial aryl group which adopted edge- or face-on orientations. The 3,5-di-*tert*-butylphenyl complex **2j** had a slightly different solid state structure. It appears that interactions of the 3,5-di-*tert*-butylphenyl substituent with the COD ligand cause the latter to be twisted out of the square plane, so much, in fact, that the complex more closely resembles a tetrahedral structure. We conclude from these observations that within the series of complexes that were examined by X-ray crystallography, ligand **1j** imposes the most serious steric demands on the metal. In the catalysis experiments, complex **2j** was one of the more enantioselective catalysts (see below).

**Hydrogenation reactions:** These reactions were performed in parallel by placing several tubes in a Parr autoclave and running the hydrogenations simultaneously. Critical data for hydrogenation of *E*-1,2-diphenylpropene are shown in Figure 2, and Table 1 gives more details. The complex with the smallest R<sup>1</sup> substituent, the methyl-oxazoline complex **2a**, gave a high yield of product but the enantiomeric excess was modest (63%). Substitution of the methyl group with a *tert*-butyl decreased the yield but increased the enantioselectivity. Complexes **2a** and **2b** both have diphenylphosphino P centers, whereas the *tert*-butyl complex **2c** has a di(2-methylphenyl)phosphino group. This change resulted in a lower yield but a higher enantioselectivity. Complex **2d** (R<sup>1</sup> = 1-Ad, R<sup>2</sup> = Ph) gave a very poor yield and a reasonable enantioselectivity (slightly increased yield was obtained when the reaction was run at -5 °C under 70 bar H<sub>2</sub>). However, when the R<sup>1</sup> substituent was very large, as in complex **2e** (R<sup>1</sup> = CPh<sub>3</sub>), both the yield and the enantioselectivity of the reaction were greatly diminished.

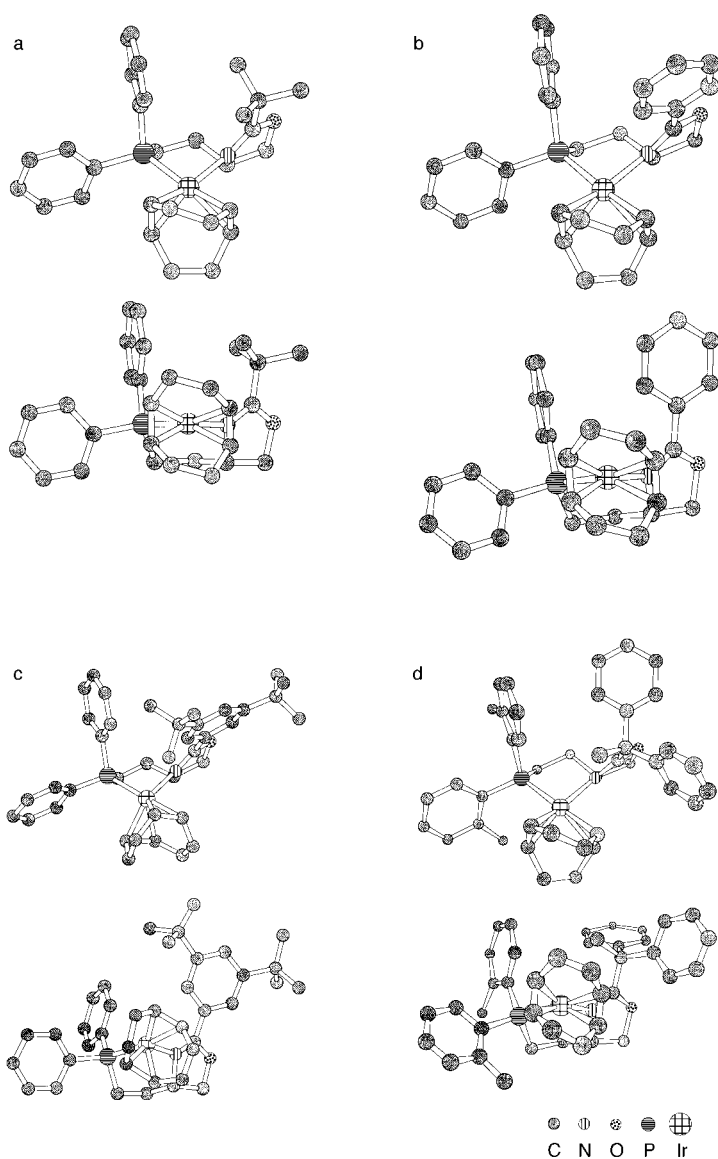


Figure 1. Top and side views of a) [(cod)Ir**1b**]BARF; b) [(cod)Ir**1i**]PF<sub>6</sub>; c) [(cod)Ir**1j**]PF<sub>6</sub>; and d) [(cod)Ir**1h**]BARF. All diagrams generated from X-ray coordinates and presented in Chem3D. Counterions are omitted for clarity throughout.

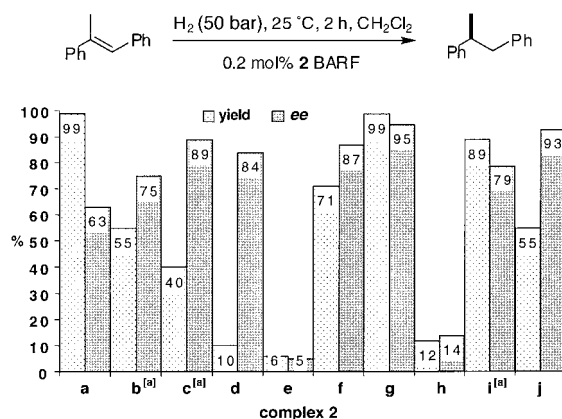


Figure 2. Enantioselectivity and yield data as a function of the ligand used in the reactions shown. [a] 0.1 mol% of catalyst was used.

We hypothesized that a diphenylmethyl R<sup>1</sup> substituent might be advantageous for the following reasons. A diphenylmethyl substituent is large and non-spherical and, unlike the CPh<sub>3</sub> group it can adopt conformations that accommodate the substrates on the metal by placing the two phenyls away from the metal. Moreover, the two phenyl groups could adopt an edge-face conformation (Figure 3a) reminiscent of that in complexed, optically active, C<sup>2</sup> symmetric phosphines and some other ligand types (Figure 3b).<sup>[17]</sup> We were unable to crystallize the HCPH<sub>2</sub> derivative **2g** for X-ray crystallographic analysis. However, the solid state structure of complex **2h** (R<sup>1</sup> = MeCPh<sub>2</sub>) shows that its phenyl groups adopt a conformation which resembles the edge-face motif (Figure 3c).

Complex **2f** (R<sup>1</sup> = CHPh<sub>2</sub>, R<sup>2</sup> = Ph) gave a higher enantioselectivity than the corresponding methyl (**2a**), *tert*-butyl (**2b**), and 1-adamantyl complexes (**2d**), thus supporting the hypothesis outlined above. We then looked for another factor that could be changed to further increase the enantioselectivity. The observation that the diphenylphosphino coordinating group in complex **2b** gave an inferior result to the di(2-methylphenyl)phosphino complex **2c** in the R<sup>1</sup> = *tert*-butyl series implied that this change might be more generally

Table 1. Enantioselective hydrogenation of *E*-1,2-diphenylpropene.

	Complex cation	Anion	Catalyst equiv [mol %]	<i>T</i> [°C]	<i>t</i> [h]	H <sub>2</sub> pressure [bar]	Yield <sup>[a]</sup> [%]	<i>ee</i> <sup>[b]</sup> [%]
1	<b>2a</b>	BARF	0.2	25	2	50	99	63
2	<b>2b</b>	BARF	0.1	25	2	50	55	75
3	<b>2c</b>	BARF	0.1	25	2	50	40	89
4	<b>2d</b>	BARF	0.2	25	2	50	10	84
5	<b>2e</b>	BARF	0.1	25	2	59	6	5
6	<b>2f</b>	BARF	0.2	25	2	50	71	87
7	<b>2g</b>	BARF	0.2	25	2	50	99	95
8	<b>2h</b>	BARF	0.2	25	2	50	12	14
9	<b>2i</b>	BARF	0.1	25	2	50	89	79
10	<b>2i</b>	PF <sub>6</sub> <sup>-</sup>	0.1	25	2	50	5	28
11	<b>2i</b>	BARF <sup>[c]</sup>	0.1	25	2	50	96	79
12	<b>2j</b>	BARF <sup>[c]</sup>	0.2	25	2	50	55	93
13	<b>2b</b>	BARF	0.1	-5	2	50	37	90
14	<b>2b</b>	BARF	0.2	-5	2	50	37	87
15	<b>2b</b>	BARF	0.4	-5	2	50	35	88
16	<b>2b</b>	BARF	0.2	-5	2	70	45	90
17	<b>2b</b>	BARF	0.2	-5	20	70	42	89
18	<b>2d</b>	BARF	0.2	-5	2	70	58	82

[a] GLC yield. [b] Enantiomeric excess was determined by GLC (100 °C, retention time:  $t_1 = 117.6$  min,  $t_2 = 120.9$  min). [c] 1 mol % of NaBARF [BARF = tetrakis[3,5-bis(trifluoromethyl)phenyl]borate] was added.

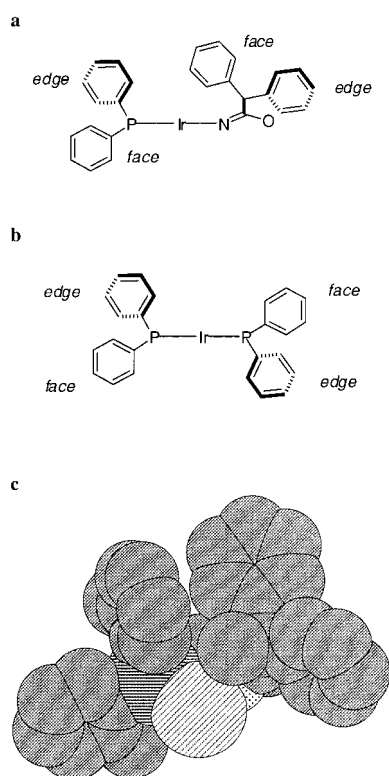


Figure 3. a) Anticipated edge-face orientation of phenyl groups in complex **2g**; b) edge-face orientation of phenyl groups in a typical  $C_2$ -symmetric chiral phosphine complex; and, c) Chem3D space filling model of the  $[\text{Ir}1\text{h}]^+$  fragment of the complex **2h** generated from X-ray crystallographic coordinates.

beneficial. Indeed, complex **2g** ( $R^1 = \text{CHPh}_2$ ,  $R^2 = 2\text{-MeC}_6\text{H}_4$ ) gave the best data under these conditions. The extreme sensitivity of the catalysis to the  $R^1$  substituent became

evident when complex **2h** ( $R^1 = \text{CMePh}_2$ ,  $R^2 = 2\text{-MeC}_6\text{H}_4$ ) was tested. Substitution of the methine hydrogen with a methyl group in the  $R^1$  substituent caused a marked reduction in the catalytic effectiveness in terms of both yield and enantiomeric excess.

Complex **2i** is different to **2a–2h** insofar as the  $R^1$  phenyl-substituent in this complex is planar. In the hydrogenation reaction, complex **2i** gave a good yield and a moderately good enantiomeric excess, and complex **2j** gave slightly better data (Table 2, entries 16 and 17).

Pfaltz and co-workers had discovered that the BARF counterion<sup>[18, 19]</sup> was critical in their hydrogenation studies for obtaining good yields. They have measured conversion as a function of reaction time and from this deduced that catalyst deactivation was a serious problem for other counterions such as  $\text{PF}_6^-$ . The same factors are operative in the reactions studied here. For instance, if the hexafluorophosphate salt of cation **2i** was used, then the yield dropped precipitously (Table 1, compare entries 9 and 10). The presence of  $\text{PF}_6^-$  is not intrinsically detrimental to this reaction because when 10 equivalents of NaBARF were added to a reaction mediated by **2i** $\text{PF}_6^-$ , the yield was slightly better than observed for the corresponding BARF complex, and the enantioselectivity was the same (entries 11 and 9). When the  $\text{PF}_6^-$  salt of complex **2j** was screened using 10 equivalents of NaBARF in the same way, a good enantioselectivity was obtained but the yield was only 55%.

Yields and enantioselectivities in these reactions depend on several variables; this was illustrated in a series of experiments involving complex **2b**. When the experiment in entry 2 was repeated but at  $-5^\circ\text{C}$  rather than  $25^\circ\text{C}$ , the enantioselectivity increased by 15%, but the yield fell by 18% (Table 1, entries 2 and 13). Catalyst concentration over the range 0.1–0.4 mol % had little effect at  $-5^\circ\text{C}$  (entries 13–15). Both the

yields and the enantioselectivities marginally increased when the pressure was increased from 50 to 70 bar (entries 14 and 16). Prolonged reaction times, however, did not increase the yield (entries 16 and 17).

Figure 4 and Table 2 summarize the data for hydrogenation of a similar, but more electron-rich substrate, *E*-2-(methoxyphenyl)-1-phenylpropene. The methyl-oxazoline complex **2a** gave a good yield and enantioselectivity considering this

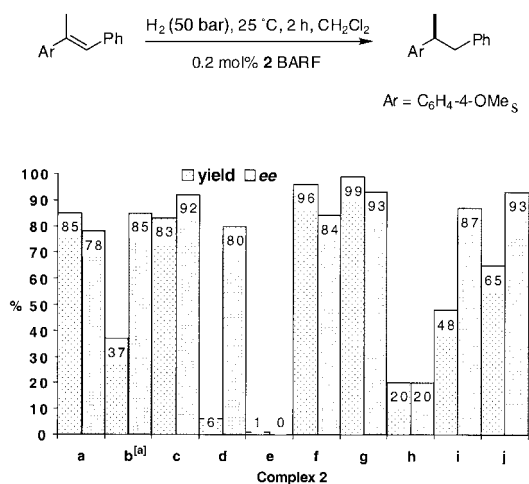


Figure 4. Enantioselectivity and yield data as a function of the ligands used in the reaction shown. [a] 0.1 mol % of catalyst was used.

substituent is so small, and that the reaction was run at 25 °C (Table 2, entry 1). Complex **2b** has the larger, *tert*-butyl, substituent, and higher enantioselectivities were observed for this (up to 91 %, entry 7). However, for both catalysts **2a** and **2b**, it was difficult to drive the reactions to completion.

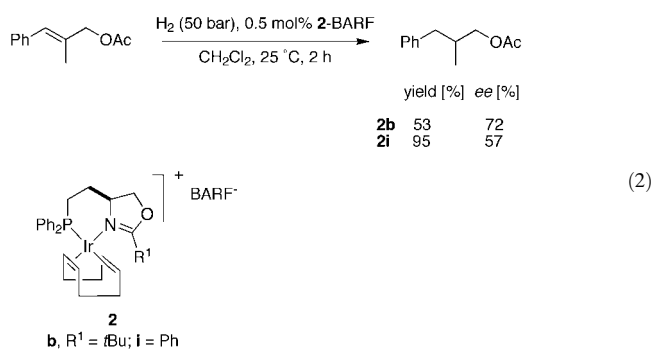
Table 2. Enantioselective hydrogenation of 1-phenyl-2-(4-methoxyphenyl)propene.

Complex cation	Catalyst equiv (mol %)	<i>T</i> [°C]	<i>t</i> [h]	H <sub>2</sub> pressure [bar]	Yield <sup>[a]</sup> [%]	<i>ee</i> <sup>[b]</sup> [%]
1 <b>2a</b>	0.3	25	2	50	85	78
2 <b>2b</b>	0.1	25	2	50	37	85
3 <sup>c</sup> <b>2b</b>	0.1	25	2	50	15	68
4 <b>2b</b>	0.1	-5	2	50	50	88
5 <b>2b</b>	0.2	-5	2	50	64	84
6 <b>2b</b>	0.4	-5	2	50	61	78
7 <b>2b</b>	0.2	-5	2	70	63	91
8 <b>2b</b>	0.2	-5	20	70	62	88
9 <b>2c</b>	0.2	-5	2	70	92	94
10 <b>2c</b>	0.3	25	2	50	83	92
11 <b>2d</b>	0.2	25	2	50	6	80
12 <b>2e</b>	0.3	25	2	50	1	0
13 <b>2f</b>	0.3	25	2	50	96	84
14 <b>2g</b>	0.3	25	2	50	99	93
15 <b>2h</b>	0.3	25	2	50	20	20
16 <b>2i</b>	0.3	25	2	50	48	87
17 <b>2j</b>	0.3	25	2	50	65	93

[a] GLC yield. [b] The enantiomeric excess was determined by GLC (130 °C, retention time: *t*<sub>1</sub> = 101.7 min, *t*<sub>2</sub> = 105.0 min). [c] Acetone (0.2 μL, 0.4 equiv catalyst) was added.

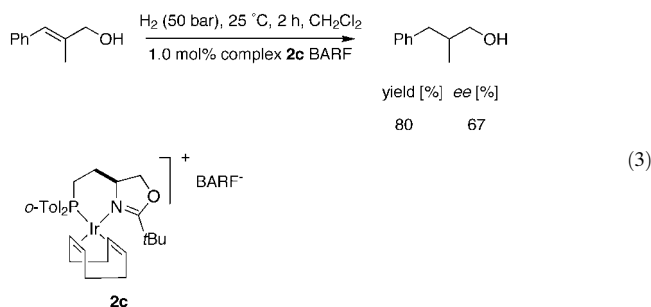
Comparison of entries 2 and 3 shows that the reaction system is extremely sensitive to extraneous coordinating groups. A small amount of acetone was deliberately added in the second of these experiments, and both the yield and the enantioselectivity decreased. Similar observations were made by Crabtree for his catalyst.<sup>[20]</sup> Entries 7 and 8 describe identical experiments except that the reaction time was longer in the latter case. Comparable data were obtained implying that the catalyst had ceased to function after approximately 2 h in both experiments. Collectively, these observations indicate that the size of the substituents R<sup>1</sup> and R<sup>2</sup> influence the catalyst stability. Indeed, the more hindered di(2-methylphenyl)phosphino-complex **2c** gave better conversions than the diphenylphosphino-derivative **2b**. The adamantyl complex **2d** gave similar enantioselectivities to the closely related *tert*-butyl complex **2b** but lower yields. Just as in the last set of experiments, the triphenylmethyl oxazoline complex **2e** gave very poor conversions and enantioselectivities, but the diphenylmethyl complex **2f** gave much better data (entries 12 and 13). Superior to that, and the best result in the series, the corresponding di(2-methylphenyl)phosphino complex **2g** gave good conversion and enantioselectivity (entry 14) at room temperature and a lower pressure than in the second best experiment (entry 9). Again, the 1,1-diphenylethyl complex **2h** did not perform as well as the corresponding diphenylmethyl complex **2g** (entries 14 and 15). The two complexes with relatively flat R<sup>1</sup> substituents, **2i** and **2j**, did not perform as well as the ones with more three dimensional groups (entries 16 and 17).

3-Acetoxy-2-methylphenylpropene was screened by a strategy which was similar to those outlined above. Details of these experiments are given in the Supporting Information. The best data are shown in Reaction (2). Two complexes gave



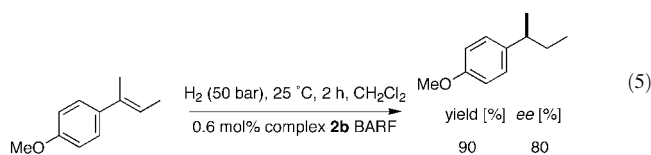
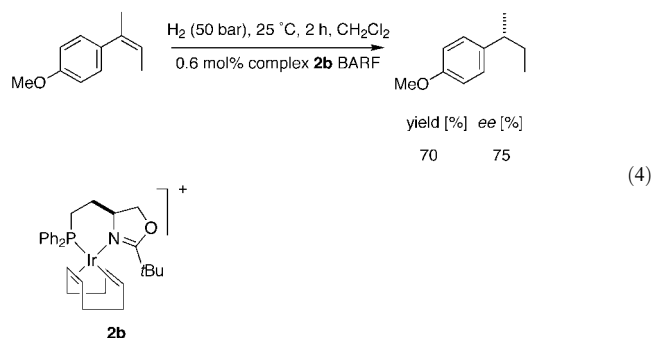
moderately good results. The *tert*-butyl complex **2b** gave the highest enantioselectivity in the series, but only 53 % conversion to product, whereas the phenyloxazoline complex **2i** gave 15 % less enantioselectivity but a good yield. The corresponding allylic alcohol behaved similarly [Reaction (3)].

Unlike the data obtained for the first two substrates, the results shown above are significantly inferior to that reported by Pfaltz.<sup>[12]</sup> Two extreme modifications were attempted to improve the performance of our catalysts, but neither worked. For instance, hydrogenations using the phenyl-oxazoline



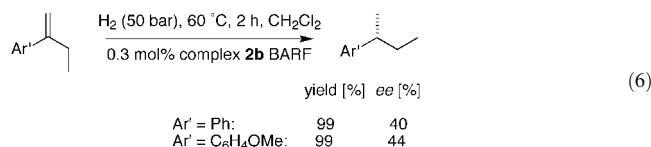
complex **2i**BARF in the presence of Cs<sub>2</sub>CO<sub>3</sub> or NEt<sub>3</sub><sup>[21]</sup> gave low yields of product with poor enantioselectivities (< 8%). A reaction using complex **2c**BARF in the ionic liquid<sup>[22–27]</sup> *N,N'*-ethylmethylimidazolium tetrafluoroborate gave no conversion to product.

Reactions (4) and (5) show our two best results for hydrogenation of 2-aryl-2-butene derivatives. On an absolute scale, the conversions and enantioselectivities were good but not excellent. The enantioselectivities obtained in Reaction (4) were better than those reported for iridium complexes of ligand **A**,<sup>[12, 13]</sup> but not as good as those reported for ligand **B**<sup>[28]</sup> for the same substrate. Similar trends were observed for the corresponding *trans*-alkene substrate [Reaction (5)]. The absolute configuration of the hydrogenation products in Reactions (4) and (5) were opposite; Pfaltz and co-workers observed the same phenomenon in their studies.<sup>[12]</sup>



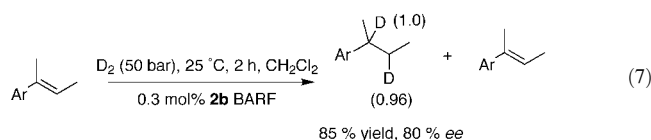
Finally, two 1,1-disubstituted alkenes were investigated, and the best data are shown in Reaction (6). Interestingly, the enantioselectivities increased slightly when the reactions were run at 60 °C rather than –5 or 25 °C (see Supporting Information). In absolute terms, the *ee* values shown are not high. However, 1,1-disubstituted alkenes are notoriously difficult to hydrogenate with high enantioselectivities, and the data shown here compare favorably with those reported for other catalysts.

**Deuterium labeling experiments:** The data presented above prove that enantioselective hydrogenations of 1,2-diaryl

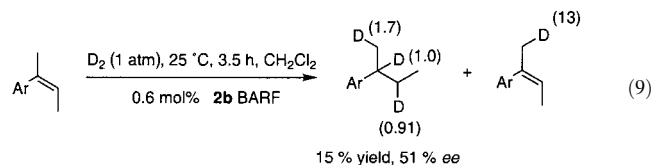
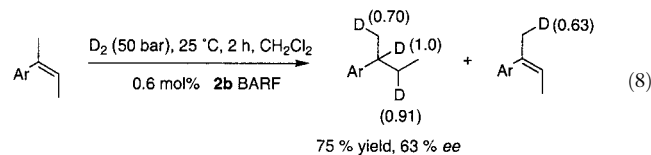


propene derivatives are the easiest to effect. Lesser enantioselectivities for the other substrates probably reflect non-ideal enantiodiscrimination by the catalyst. However, we became suspicious that another contributing factor might be operative: double bond migrations at rates that are competitive with the desired hydrogenation reactions. To check this possibility, a series of deuteration experiments were performed. Some typical data from these experiments are shown in Figure 5.

The first experiment did not provide evidence for double bond migration. Thus when *E*-2-(4-methoxyphenyl)-2-butene was deuterated under the conditions shown in Reaction (7), deuterium atoms were detected only in the positions where the double bonds were previously located. GC/MS experiments indicated that only two deuteriums were incorporated into the product.



Deuteration of the *cis*-substrate, *Z*-2-(4-methoxyphenyl)-2-butene, gave a different result to deuteration of the *trans*-substrate [Reactions (8) and (7)]. The distribution of deuterium atoms in the product implies that extensive double bond migration occurred before the hydrogenation step. Interestingly, the reaction did not go to completion and the recovered starting material had deuterium incorporated at the methyl group shown, but the *Z*-stereochemistry of the double bond was retained and no double bond migration product was observed. GC/MS analyses indicated that the reduced product contained 2–4 deuterium atoms. More deuterated starting material was observed when the reaction was performed under only 1 atm of D<sub>2</sub> [Reaction (9)].



Deuteration of 2-(4-methoxyphenyl)-1-butene also showed that extensive double bond migration had occurred [Reac-

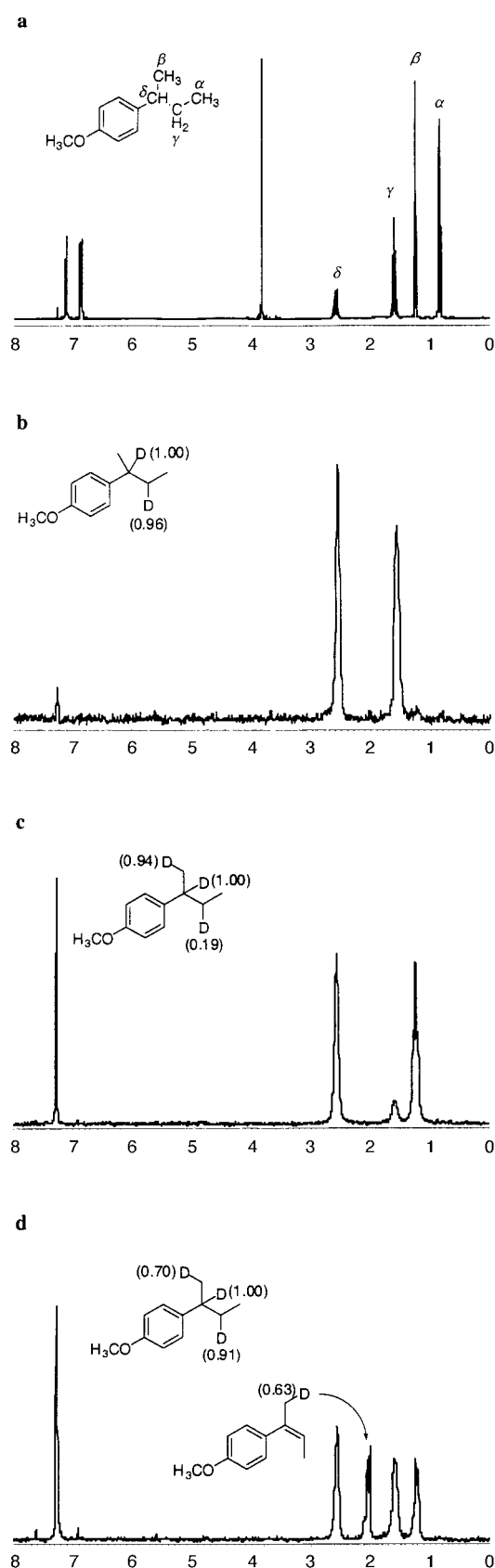
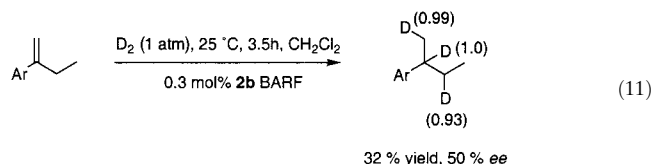
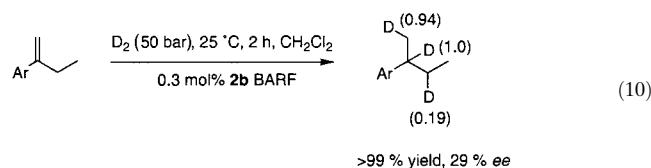


Figure 5. Typical data from deuterium labeling studies: a)  $^1\text{H}$  NMR spectrum of 2-(4-methoxy)phenylbutane; b)  $^2\text{H}$  NMR of the crude material from the reaction of 50 bar  $\text{D}_2$  with *E*-2-(4-methoxy)phenyl-2-butene; c)  $^2\text{H}$  NMR of the crude material from the reaction of 50 bar  $\text{D}_2$  and 2-(4-methoxy)phenylbut-1-ene; d)  $^2\text{H}$  NMR of the crude material from the reaction of 50 bar  $\text{D}_2$  and *Z*-2-(4-methoxy)phenyl-2-butene.

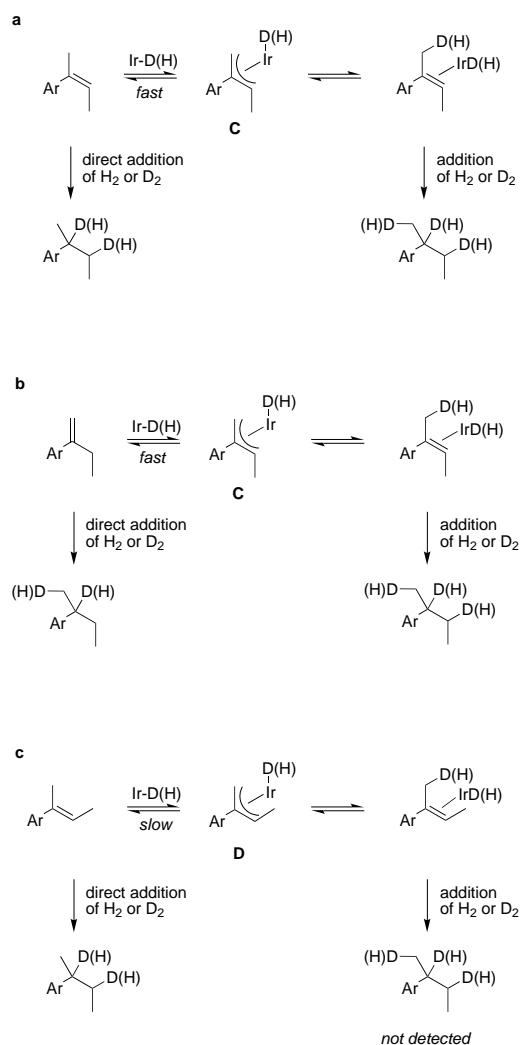
tion (10)]. The reduced product containing 2–4 deuterium atoms was detected in GC/MS experiments. Under 1 atm of  $\text{D}_2$  this more reactive substrate was almost totally converted to product, also with scrambling of the deuterium label (Reaction 11).



Two interesting questions arise from the deuterium incorporation experiments. First, how do the double bond migration reactions occur? Second, why do they occur for the *cis*-alkene shown in Reaction (8) but not the *trans*-isomer in Reaction (7)? The data collected does not allow us to answer these questions with complete certainty, but the working hypothesis expressed in Scheme 1 accounts for all the observations made. We propose the labeling in Reactions (8) and (9) is consistent with formation of an allyl intermediate **C**. Insertion, and deuteration/hydrogenation of the double bond accounts for the label distribution observed (Scheme 1a). Similarly, involvement of the  $\pi$ -allyl complex **C** explains the label distribution observed in Reaction (10) (Scheme 1b). However, if this proposal is valid, then there must be a factor that accounts for lack of scrambling via a similar intermediate,  $\pi$ -allyl **D**, in Reaction (7). Complexes **C** and **D** are stereoisomers, and **D** is likely to be the least stable of the two. Therefore, Hammond postulate leads to the conclusion that **D** will form more slowly than **C**, and we propose that this difference is such that formation of **C** is competitive with the hydrogenation reaction whereas **D** is not.

## Conclusion

Double bond migration competing with the hydrogenation reactions is an important, though unwelcome, observation. If a substrate partially isomerizes before it reacts, then asymmetric reduction of both alkenes must be controlled to obtain high enantioselectivities. This is a difficult thing to achieve. Consequently, modifications to improve the enantioselectivities of iridium-mediated hydrogenations of the type described here must involve methods to suppress double bond migration and/or enhance the relative rate of the direct reduction step. The importance of double bond migration in these hydrogenations mediated by chiral derivatives of Crabtree's catalyst has not been noted before this work, even though similar effects have been thoroughly investigated for hydrogenation of allylic alcohols mediated by ruthenium-BINAP catalysts.<sup>[13, 29, 30]</sup>



Scheme 1. Working hypothesis for the incorporation of deuterium in the labeling experiments: a) for Reaction (8); b) for Reaction (10); and c) for Reaction (7).

Double bond migration reactions have been observed in hydrogenation/deuteration of pinene derivatives using Crabtree's catalysts itself.<sup>[31]</sup>

The possibility of competing double bond migration reactions also makes the data from the enantioselective reactions harder to compare. If one ligand gives a higher enantioselectivity than another, we cannot be sure that this is because the design of the first ligand is more conducive to asymmetric induction in the desired reaction rather than diminished competing migration reactions.

The yield and enantioselectivity data in this paper does prove that ligands **1** in complexes **2** can act as highly enantioselective hydrogenation catalysts. Optimization of these involves the topography of the R<sup>1</sup> substituent. If R<sup>1</sup> is too large, or has an inappropriate shape, the rate of the desired hydrogenation process might be suppressed relative to catalyst degradation, adversely affecting the conversions. Substitution of the phosphine Ph substituents with 2-MeC<sub>6</sub>H<sub>4</sub>, however, tends to increase the enantioselectivities without decreasing conversions. The strategy expressed in Figure 2 for optimization of enantioselectivities by incorporation of

HCAr<sub>2</sub> groups at critical positions was helpful here, and may be useful in other cases. Development of asymmetric hydrogenation reactions to give uniformly high enantiomeric excesses for a variety of alkene substrates will hinge on careful consideration of issues such as these in conjunction with modifications to suppress competing double bond migration.

## Experimental Section

**General procedures:** High field NMR spectra were recorded on Varian Unity Plus 300 (<sup>1</sup>H at 300 MHz, <sup>13</sup>C at 75 MHz, <sup>2</sup>H at 46 MHz, and <sup>31</sup>P at 121 MHz) spectrometers. Chemical shifts of <sup>1</sup>H and <sup>13</sup>C spectra are referenced to the NMR solvents; <sup>31</sup>P spectra are referenced to H<sub>3</sub>PO<sub>4</sub> (85%) external standard (δ = 0). Melting points are uncorrected. Optical rotations were measured on Jasco DIP-360 digital polarimeter. Flash chromatography was performed using silica gel (230–600 mesh). Thin-layer chromatography was performed on glass plates coated with silica gel 60 F254 (E. Merck, Darmstadt, Germany). Elemental analyses were performed by Atlantic Microlab, Norcross, GA. CH<sub>2</sub>Cl<sub>2</sub> was distilled over CaH<sub>2</sub> and THF over Na/benzophenone. Other solvents were purchased from commercial suppliers and were used without further purification. Chloro-1,5-cyclooctadiene iridium(I) dimer was provided by Johnson Matthey. *E*-2-(4-Methoxyphenyl)-1-phenylpropene,<sup>[32]</sup> *E*- and *Z*-2-(4-methoxyphenyl)-2-butene,<sup>[33]</sup> 2-phenyl-1-butene, and 2-(4-methoxyphenyl)-1-butene were prepared according to literature procedures. Enantioselectivities were deduced through GC on a chiral support.<sup>[34]</sup>

The absolute configurations of the products were confirmed in some cases, and inferred in others as outlined below. The product in Table 1 and in Reaction (6) where Ar' = Ph is the same, and its the absolute configuration was confirmed by comparing optical rotations with those reported by Buchwald.<sup>[6]</sup> The absolute configuration of the product in the experiments listed in Table 2 and in Reactions (4)–(6) (Ar' = C<sub>6</sub>H<sub>4</sub>-4-OMe) was inferred from comparing the GC retention factors of this product with that in Table 1; this is likely to be correct since the two alkanes are so similar (differ only by a *para*-methoxy group on one aryl).

Deuterium gas under high pressure was purchased from Praxair Inc, Danbury, CT. All the ligands **1** were prepared by the method reported previously,<sup>[16]</sup> and spectroscopic data for the particular derivatives that have not been discussed before (**1a**, **1c**, **1f**, **1g** and **1h**) are given in the following sections.

**(S)-2-Methyl-4-[(diphenylphosphino)ethyl]oxazoline (1a):** *R*<sub>f</sub> = 0.27 (ethyl acetate/hexane 3:7 *v/v*); [ $\alpha$ ]<sub>D</sub><sup>25</sup> = –87.6 (*c* = +3.4, CHCl<sub>3</sub>); <sup>1</sup>H NMR (CDCl<sub>3</sub>, 300 MHz): δ = 7.48–7.43 (m, 4H), 7.37–7.33 (m, 6H), 4.30 (dd, *J* = 9, 8 Hz, 1H), 4.16 (m, 1H), 3.79 (dd, *J* = 8, 8 Hz, 1H), 2.31–2.21 (m, 1H), 2.12–2.02 (m, 1H), 1.99 (s, 3H), 1.74–1.60 (m, 2H); <sup>13</sup>C NMR (CDCl<sub>3</sub>, 75 MHz): δ = 164.7, 132.8, 132.6, 128.6–128.4, 72.3, 67.2 (d, *J*<sub>CP</sub> = 13.5 Hz), 32.1 (d, *J*<sub>CP</sub> = 16.5 Hz), 24.2 (d, *J*<sub>CP</sub> = 11.5 Hz), 13.9; <sup>31</sup>P NMR (CDCl<sub>3</sub>, 121 MHz): δ = –15.46; HRMS: *m/z*: calcd for C<sub>18</sub>H<sub>21</sub>NOP: 298.13608 [*M*+H]<sup>+</sup>; found: 298.13623.

**(S)-2-*tert*-Butyl-4-[(bis(2-tolyl)phosphino)ethyl]oxazoline (1c):** *R*<sub>f</sub> = 0.32 (ethyl acetate/hexane 1:9 *v/v*); [ $\alpha$ ]<sub>D</sub><sup>25</sup> = –79.6 (*c* = 1.0, CHCl<sub>3</sub>); <sup>1</sup>H NMR (CDCl<sub>3</sub>, 300 MHz): δ = 7.30–7.20 (m, 4H), 7.20–7.15 (m, 4H), 4.28 (dd, *J* = 9, 8 Hz, 1H), 4.19 (m, 1H), 3.88 (dd, *J* = 6, 8 Hz, 1H), 2.46 (m, 6H), 2.18–2.12 (m, 1H), 2.03–1.99 (m, 1H), 1.76–1.33 (m, 2H), 1.27 (s, 9H); <sup>13</sup>C NMR (CDCl<sub>3</sub>, 75 MHz): δ = 173.8, 142.4–141.9, 136.8–136.4, 131.0, 130.0, 128.3, 125.9, 71.9, 66.6 (d, *J*<sub>CP</sub> = 13.5 Hz), 33.0, 32.0 (d, *J*<sub>CP</sub> = 17.5 Hz), 27.8, 22.5 (d, *J*<sub>CP</sub> = 12.0 Hz), 21.0 (d, *J*<sub>CP</sub> = 21.5 Hz); <sup>31</sup>P NMR (CDCl<sub>3</sub>, 121 MHz): δ = –37.6; HRMS: *m/z*: calcd for C<sub>23</sub>H<sub>31</sub>NOP: 368.21433 [*M*+H]<sup>+</sup>; found: 368.21308.

**(S)-2-Diphenylmethyl-4-[(diphenylphosphino)ethyl]oxazoline (1f):** *R*<sub>f</sub> = 0.78 (ethyl acetate/hexane 3:7 *v/v*); [ $\alpha$ ]<sub>D</sub><sup>25</sup> = –57.5 (*c* = 4.4, CHCl<sub>3</sub>); <sup>1</sup>H NMR (CDCl<sub>3</sub>, 300 MHz): δ = 7.50–7.37 (m, 4H), 7.36–7.26 (m, 16H), 5.32 (s, 0.5H), 5.15 (s, 0.5H), 4.38–4.25 (m, 2H), 3.94 (m, 1H), 2.24–2.19 (m, 1H), 2.10–2.02 (m, 1H), 1.78–1.68 (m, 2H); <sup>13</sup>C NMR (CDCl<sub>3</sub>, 75 MHz): δ = 166.8, 139.3, 132.9, 132.6, 132.4, 128.6–128.4, 127.0, 72.2, 66.6 (d, *J*<sub>CP</sub> = 14.0 Hz), 50.9, 31.9 (d, *J*<sub>CP</sub> = 17.0 Hz), 23.6 (d, *J*<sub>CP</sub> = 11.5 Hz); <sup>31</sup>P



NMR (CDCl<sub>3</sub>, 121 MHz):  $\delta = -15.5$ ; HRMS:  $m/z$ : calcd for C<sub>30</sub>H<sub>29</sub>NOP: 450.19868 [M+H]<sup>+</sup>; found: 450.19874.

**(S)-2-Diphenylmethyl-4-[(bis(2-methylphenyl)phosphino)ethyl]oxazoline (1g):**  $R_f = 0.69$  (ethyl acetate/hexane 3:7 v/v);  $[\alpha]_D^{25} = -70.6$  ( $c = 5.7$ , CHCl<sub>3</sub>); <sup>1</sup>H NMR (CDCl<sub>3</sub>, 300 MHz):  $\delta = 7.80$ –7.30 (m, 8H), 7.29–7.15 (m, 10H), 5.17 (s, 1H), 4.40–4.31 (m, 2H), 4.16 (m, 1H), 3.96 (dd,  $J = 7$ , 6 Hz, 1H), 2.46 (s, 6H), 2.14–2.10 (m, 1H), 2.02 (m, 1H), 1.82–1.74 (m, 2H); <sup>13</sup>C NMR (CDCl<sub>3</sub>, 75 MHz):  $\delta = 167.4$ , 142.5–141.9, 139.3, 136.4, 131.0, 129.9, 128.6–128.4, 127.1, 126.0, 72.2, 66.7 (d,  $J_{C,P} = 13.5$  Hz), 50.1, 32.9 (d,  $J_{C,P} = 18$  Hz), 22.6 (d,  $J_{C,P} = 11.5$  Hz), 21.1 (d,  $J_{C,P} = 21$  Hz); <sup>31</sup>P NMR (CDCl<sub>3</sub>, 121 MHz):  $\delta = -37.3$ ; LSIMS:  $m/z$ : calcd for C<sub>32</sub>H<sub>33</sub>NOP: 478 [M+H]<sup>+</sup>; found: 478.

**(S)-2-(1,1-Diphenyl)ethyl-4-[(bis(2-methylphenyl)phosphino)ethyl]oxazoline (1h):**  $R_f = 0.82$  (ethyl acetate/hexane 3:7 v/v);  $[\alpha]_D^{25} = -68.7$  ( $c = 9.0$ , CHCl<sub>3</sub>); <sup>1</sup>H NMR (CDCl<sub>3</sub>, 300 MHz):  $\delta = 7.40$ –7.20 (m, 18H), 4.39–4.30 (m, 2H), 3.98 (m, 1H), 2.47 (s, 6H), 2.15–2.13 (m, 1H), 2.10 (s, 3H), 2.10–2.03 (m, 1H), 1.82–1.77 (m, 2H); <sup>13</sup>C NMR (CDCl<sub>3</sub>, 75 MHz):  $\delta = 170.7$ , 144.8, 142.5–141.9, 136.8–136.4, 131.1, 129.9, 128.7–128.4, 127.9, 126.6, 126.0, 72.2, 66.6 (d,  $J_{C,P} = 13.5$  Hz), 50.3, 31.9 (d,  $J_{C,P} = 18$  Hz), 28.4, 22.5 (d,  $J_{C,P} = 11.5$  Hz), 21.2 (d,  $J_{C,P} = 21$  Hz); <sup>31</sup>P NMR (CDCl<sub>3</sub>, 121 MHz):  $\delta = -37.3$ ; LSIMS:  $m/z$ : calcd for C<sub>33</sub>H<sub>35</sub>NOP: 490 [M+H]<sup>+</sup>; found: 490.

**General procedure for preparation of complex 2b (analogously 2a–2j):**<sup>[6]</sup> Ligand **1b** (48.0 mg, 0.143 mmol) and chloro-(1,5-cyclooctadiene)iridium(i) dimer (48.2 mg, 0.0717 mmol) were dissolved in CH<sub>2</sub>Cl<sub>2</sub> (3 mL) in a 10 mL flask equipped with a condenser and a stir bar. The solution was refluxed under N<sub>2</sub> for 1 h. After the orange-red solution was cooled to room temperature, NaBARF<sup>[18]</sup> (195 mg, 0.22 mmol) was added followed by H<sub>2</sub>O (2 mL), and the resulting two-phase mixture was stirred vigorously for 15 min. The layers were separated and the aqueous layer was extracted with CHCl<sub>3</sub> (2 × 10 mL). The combined organic extracts were washed with water and evaporated. The residue was re-dissolved in EtOH (1.5 mL) and crystallized by the slow addition of H<sub>2</sub>O to give **2b** (133 mg, 0.0887 mmol, 62%) as a yellow-orange solid. M.p. 162–165 °C (decomp);  $[\alpha]_D^{25} = -54.2^\circ$  ( $c = 0.5$ , CDCl<sub>3</sub>); <sup>1</sup>H NMR (CDCl<sub>3</sub>, 300 MHz):  $\delta = 7.70$  (m, 8H), 7.61–7.55 (m, 10H), 7.51–7.33 (m, 2H), 7.11–7.07 (m, 2H), 4.81 (m, 1H), 4.37 (m, 1H), 4.27–4.18 (m, 2H), 4.04 (dd,  $J = 9$ , 3 Hz, 1H), 3.91 (m, 1H), 2.88–2.72 (m, 3H), 2.48–2.43 (m, 1H), 2.32–2.23 (m, 2H), 2.15–1.91 (m, 4H), 1.76–1.59 (m, 2H), 1.42–1.39 (m, 1H), 1.10 (s, 9H); <sup>13</sup>C NMR (CDCl<sub>3</sub>, 75 MHz):  $\delta = 180.1$ , 162.7, 162.0, 161.4, 160.7, 134.7, 132.5, 131.3, 131.2–126.8, 126.3, 122.7, 119.1, 117.5, 94.8 (d,  $J = 8$  Hz), 86.5 (d,  $J = 17$  Hz), 72.5, 67.8 (d,  $J = 3$  Hz), 65.8, 64.9, 36.7 (d,  $J = 5$  Hz), 33.6, 30.1, 28.6 (d,  $J = 2$  Hz), 28.5, 25.5 (d,  $J = 3$  Hz), 23.8 (d,  $J = 34$  Hz); <sup>31</sup>P NMR (CDCl<sub>3</sub>, 121 MHz):  $\delta = 7.48$ ; elemental analysis calcd (%) for C<sub>61</sub>H<sub>50</sub>BF<sub>24</sub>IrNOP: C 48.75, H 3.35, N 0.93; found: C 48.80, H 3.39, N 0.87.

**Complex 2a:** This compound was prepared by the same method used for **2b**, but beginning with **1a** (51 mg, 0.17 mmol) and chloro-(1,5-cyclooctadiene)iridium(i) dimer (58 mg, 0.086 mmol). Complex **2a** (136.5 mg, 0.094 mmol, 55%) was produced as an orange solid. M.p. 138–141 °C (decomp);  $[\alpha]_D^{25} = +77.6^\circ$  ( $c = 0.5$ , CDCl<sub>3</sub>); <sup>1</sup>H NMR (CDCl<sub>3</sub>, 300 MHz):  $\delta = 7.78$ –7.21 (m, 20H), 7.13–7.06 (m, 2H), 4.88 (m, 1H), 4.38–4.20 (m, 2H), 4.15 (m, 1H), 4.02 (dd,  $J = 9$ , 3 Hz, 1H), 3.90 (m, 1H), 2.94–2.69 (m, 3H), 2.54–2.23 (m, 4H), 2.17 (s, 3H), 2.15–1.94 (m, 2H); 1.78–1.68 (m, 2H), 1.59–1.46 (m, 2H); <sup>31</sup>P NMR (CDCl<sub>3</sub>, 121 MHz):  $\delta = 10.9$ ; elemental analysis calcd (%) for C<sub>58</sub>H<sub>44</sub>BF<sub>24</sub>IrNOP + H<sub>2</sub>O: C 47.10, H 3.14, N 0.95; found: C 46.98, H 2.98, N 1.04.

**Complex 2c:** This compound was prepared by the same method used for compound **2b**, but beginning with **1c** (68 mg, 0.19 mmol) and chloro-(1,5-cyclooctadiene)iridium(i) dimer (63 mg, 0.094 mmol). Complex **2c** (196 mg, 0.128 mmol, 68%) was produced as an orange solid. M.p. 169–171 °C (decomp);  $[\alpha]_D^{25} = -16.3^\circ$  ( $c = 3.0$ , CDCl<sub>3</sub>); <sup>1</sup>H NMR (CDCl<sub>3</sub>, 300 MHz):  $\delta = 8.05$  (br, 1H), 7.74 (s, 8H), 7.55 (s, 4H), 7.50–7.20 (m, 7H), 4.79 (br, 1H), 4.38 (m, 2H), 4.36 (m, 1H), 3.97 (m, 2H), 2.98 (br, 3H), 2.71 (br, 1H), 2.48 (br, 1H), 2.26 (m, 3H), 2.22–1.88 (m, 8H), 1.53 (br, 9H), 1.50–1.25 (m, 2H), 1.07 (br, 1H); <sup>31</sup>P NMR (CDCl<sub>3</sub>, 121 MHz):  $\delta = 21.5$  (br), 11.5 (br), 0.3; elemental analysis calcd (%) for C<sub>63</sub>H<sub>54</sub>BF<sub>24</sub>IrNOP: C 49.42, H 3.55, N 0.91; found: C 49.69, H 3.68, N 1.00. The NMR spectra of this complex appear to be broadened by a slow exchange mechanism.

**Complex 2d:** This compound was prepared by the same method used for compound **2b**, but beginning with **1d** (42 mg, 0.10 mmol) and chloro-(1,5-cyclooctadiene)iridium(i) dimer (34 mg, 0.50 mmol). Complex **2d** (69 mg,

0.043 mmol, 43%) was produced as a yellow solid. M.p. 81–84 °C (decomp);  $[\alpha]_D^{25} = -15.2^\circ$  ( $c = 1.7$ , CDCl<sub>3</sub>); <sup>1</sup>H NMR (CDCl<sub>3</sub>, 300 MHz):  $\delta = 7.76$ –7.29 (m, 20H), 7.21–7.14 (m, 2H), 4.88 (m, 1H), 4.39–4.33 (m, 2H), 4.26 (t,  $J = 9$  Hz, 1H), 4.05 (dd,  $J = 9$ , 3 Hz, 1H), 3.99 (m, 1H), 2.94 (m, 1H), 2.86–2.68 (m, 2H), 2.49 (m, 1H), 2.40 (s, 1H), 2.37–2.33 (m, 2H), 2.19–2.05 (m, 2H), 1.98–1.96 (m, 3H), 1.86 (s, 1H), 1.79 (s, 5H), 1.72 (s, 2H), 1.66–1.62 (m, 1H), 1.57–1.38 (m, 5H), 1.31–1.29 (m, 2H); <sup>31</sup>P NMR (CDCl<sub>3</sub>, 121 MHz):  $\delta = 6.9$ ; elemental analysis calcd (%) for C<sub>67</sub>H<sub>56</sub>BF<sub>24</sub>IrNOP: C 50.90, H 3.57, N 0.89; found: C 51.64, H 3.72, N 0.84.

**Complex 2e:** This compound was prepared by the same method used for compound **2b**, but beginning with **1e** (75 mg, 0.142 mmol) and chloro-(1,5-cyclooctadiene)iridium(i) dimer (48 mg, 0.071 mmol). Complex **2e** (94 mg, 0.055 mmol, 39%) was produced as a dark yellow solid. M.p. 177–179 °C (decomp);  $[\alpha]_D^{25} = -58.2^\circ$  ( $c = 2.3$ , CDCl<sub>3</sub>); <sup>1</sup>H NMR (CDCl<sub>3</sub>, 300 MHz):  $\delta = 7.76$ –7.17 (m, 32H), 6.99–6.89 (m, 5H), 4.95 (m, 1H), 4.75 (m, 1H), 4.58 (t,  $J = 9$  Hz, 1H), 4.41 (dd,  $J = 10$ , 4 Hz, 1H), 3.43 (m, 2H), 2.83 (m, 1H), 2.66–2.53 (m, 2H), 2.43–2.36 (m, 1H), 2.24–2.13 (m, 2H), 2.01 (m, 1H), 1.87 (m, 1H), 1.74 (m, 1H), 1.28–1.17 (m, 1H), 1.15–1.04 (m, 2H); <sup>31</sup>P NMR (CDCl<sub>3</sub>, 121 MHz):  $\delta = -1.5$ ; elemental analysis calcd (%) for C<sub>76</sub>H<sub>56</sub>BF<sub>24</sub>IrNOP: C 54.04, H 3.34, N 0.83; found: C 54.06, H 3.39, N 0.79.

**Complex 2f:** This compound was prepared by the same method used for compound **2b**, but beginning with **1f** (40 mg, 0.089 mmol) and chloro-(1,5-cyclooctadiene)iridium(i) dimer (30 mg, 0.044 mmol). Complex **2f** (68 mg, 0.043 mmol, 48%) was produced as an orange-red solid. M.p. 78–81 °C (decomp);  $[\alpha]_D^{25} = -14.2^\circ$  ( $c = 2.6$ , CDCl<sub>3</sub>); <sup>1</sup>H NMR (CDCl<sub>3</sub>, 300 MHz):  $\delta = 7.74$  (m, 8H), 7.63–7.29 (m, 17H), 7.24–7.18 (m, 3H), 7.10–7.06 (m, 3H), 6.48–6.46 (m, 1H), 5.43 (s, 1H), 4.86 (br, 1H), 4.65 (t,  $J = 9$  Hz, 1H), 4.40 (m, 1H), 4.27 (m, 1H), 4.18 (m, 1H), 4.10 (m, 1H), 2.98–2.87 (m, 2H), 2.80–2.50 (m, 1H), 2.57–2.45 (m, 2H), 2.39–2.17 (m, 3H), 1.96–1.70 (m, 3H), 1.50–1.29 (m, 2H); <sup>31</sup>P NMR (CDCl<sub>3</sub>, 121 MHz):  $\delta = 9.9$ ; elemental analysis calcd (%) for C<sub>70</sub>H<sub>52</sub>BF<sub>24</sub>IrNOP + H<sub>2</sub>O: C 51.54, H 3.34, N 0.86; found: C 51.32, H 3.58, N 0.83.

**Complex 2g:** This compound was prepared by the same method used for compound **2b**, but beginning with **1g** (55 mg, 0.115 mmol) and chloro-(1,5-cyclooctadiene)iridium(i) dimer (39 mg, 0.058 mmol). Complex **2g** (107 mg, 0.065 mmol, 57%) was produced as an orange-red solid. M.p. 76–79 °C (decomp);  $[\alpha]_D^{25} = -26.8^\circ$  ( $c = 3.0$ , CDCl<sub>3</sub>); <sup>1</sup>H NMR (CDCl<sub>3</sub>, 300 MHz):  $\delta = 7.80$ –7.10 (m, 24H), 6.57 (br, 2H), 5.65 (s, 1H), 4.98 (m, 1H), 4.64 (m, 2H), 4.40–4.30 (m, 1H), 4.29–4.21 (m, 1H), 4.04 (br, 1H), 3.88 (br, 1H), 3.11–2.82 (m, 4H), 2.50 (m, 1H), 2.42–2.34 (m, 2H), 2.21–2.14 (m, 1H), 1.97–1.85 (m, 3H), 1.70–1.51 (br, 3H), 1.48–1.26 (m, 2H); <sup>31</sup>P NMR (CDCl<sub>3</sub>, 121 MHz):  $\delta = 19.6$  (br), 11.7, 0.4 (br); elemental analysis calcd (%) for C<sub>72</sub>H<sub>56</sub>BF<sub>24</sub>IrNOP + H<sub>2</sub>O: C 52.12, H 3.52, N 0.84; found: C 51.82, H 3.42, N 0.91. The NMR spectra of this complex appear to be broadened by a slow exchange mechanism.

**Complex 2h:** This compound was prepared by the same method used for compound **2b**, but beginning with **1h** (80 mg, 0.16 mmol) and chloro-(1,5-cyclooctadiene)iridium(i) dimer (55 mg, 0.080 mmol). Complex **2h** (160 mg, 0.097 mmol, 60%) was produced as an orange-red solid. M.p. 173–176 °C (decomp);  $[\alpha]_D^{25} = -87.3^\circ$  ( $c = 2.6$ , CDCl<sub>3</sub>); <sup>1</sup>H NMR (CDCl<sub>3</sub>, 300 MHz):  $\delta = 8.01$ –7.10 (m, 27H), 6.77 (br, 1H), 6.52 (br, 1H), 6.09 (br, 1H), 4.62 (br, 1H), 4.50–4.39 (2H), 4.27 (1H), 4.10 (1H), 3.51 (1H), 3.20 (m, 2H), 2.98 (3H), 2.82 (3H), 2.36 (2H), 2.22 (m, 5H), 1.98–1.90 (m, 2H), 1.72 (2H), 1.58 (1H), 1.36–1.25 (m, 2H); <sup>31</sup>P NMR (CDCl<sub>3</sub>, 121 MHz):  $\delta = 20.6$  (br), 11.1 (br), -0.4; elemental analysis calcd (%) for C<sub>73</sub>H<sub>58</sub>BF<sub>24</sub>IrNOP: C 52.97, H 3.53, N 0.85; found: C 53.12, H 3.51, N 0.89. The NMR spectra of this complex appear to be broadened by a slow exchange mechanism.

**Complex 2i:** This compound was prepared by the same method used for compound **2b**, but beginning with **1i** (54 mg, 0.15 mmol) and chloro-(1,5-cyclooctadiene)iridium(i) dimer (50 mg, 0.075 mmol). Complex **2i** (149 mg, 0.098 mmol, 65%) was produced as an orange-yellow solid. M.p. 149–151 °C (decomp);  $[\alpha]_D^{25} = +10.4^\circ$  ( $c = 3.0$ , CDCl<sub>3</sub>); <sup>1</sup>H NMR (CDCl<sub>3</sub>, 300 MHz):  $\delta = 8.58$ –8.54 (m, 2H), 7.75–7.39 (m, 23H), 7.21–7.14 (m, 2H), 4.85 (m, 1H), 4.65–4.55 (m, 2H), 4.30–4.24 (m, 2H), 3.76 (m, 1H), 3.02–2.96 (m, 1H), 2.90–2.81 (m, 2H), 2.66–2.57 (m, 1H), 2.47–2.31 (m, 2H), 2.24–2.18 (m, 2H), 2.04–1.99 (m, 1H), 1.89–1.59 (m, 2H), 1.59–1.49 (m, 2H); <sup>31</sup>P NMR (CDCl<sub>3</sub>, 121 MHz):  $\delta = 9.2$ ; elemental analysis calcd (%) for C<sub>65</sub>H<sub>46</sub>BF<sub>24</sub>IrNOP: C 49.68, H 3.04, N 0.92; found: C 49.69, H 3.15, N 1.07.

**Complex 2j:** This compound was prepared by the same method used for compound **2b**, but beginning with **1j** (58 mg, 0.123 mmol), chloro-(1,5-cyclooctadiene)iridium(i) dimer (41 mg, 0.061 mmol) and ammonia hexafluorophosphate (400 mg, 2.48 mmol). Complex **2j** (65 mg, 0.071 mmol, 58%) was produced as an orange-red solid. M.p. 206–208 °C (decomp);  $[\alpha]_D^{25} = +41.0^\circ$  ( $c = 0.5$ ,  $\text{CDCl}_3$ );  $^1\text{H NMR}$  ( $\text{CDCl}_3$ , 300 MHz):  $\delta = 8.09$  (s, 1H), 7.78–7.71 (m, 3H), 7.63–7.40 (m, 7H), 7.37–7.25 (m, 2H), 5.11 (m, 1H), 4.94–4.87 (m, 2H), 4.37 (dd,  $J = 4$  Hz,  $J = 9$  Hz, 1H), 3.97 (m, 1H), 3.82 (m, 1H), 3.29–3.23 (m, 2H), 2.99–2.90 (m, 2H), 2.73–2.55 (m, 2H), 2.55–2.42 (m, 1H), 2.42–2.35 (m, 2H), 2.21–2.02 (m, 3H), 1.87–1.79 (m, 1H), 1.72–1.58 (m, 5H), 1.40–1.25 (m, 13H);  $^{31}\text{P NMR}$  ( $\text{CDCl}_3$ , 121 MHz):  $\delta = 10.9$ ,  $-143.6$  ( $J_{\text{PF}} = 710$  Hz); elemental analysis calcd (%) for  $\text{C}_{39}\text{H}_{50}\text{F}_6\text{IrNOP}_2$ : C 51.08, H 5.50, N 1.53; found: C 50.54, H 5.67, N 1.52.

**Alternative procedure for the preparation of the complexes:** Recent work has shown the following procedure can give improved yields of product complexes. The ligand (0.5 mmol) was dissolved in  $\text{CH}_2\text{Cl}_2$  (10 mL) in a glove box was added on to a stirred solution of  $[\text{Ir}(\text{cod})\text{Py}_2]\text{PF}_4$  (0.302 g, 0.5 mmol). The yellow reaction mixture was stirred for 2 h at 25 °C. The  $^{31}\text{P NMR}$  spectrum of a small aliquot indicated the complete conversion of the reaction mixture, as evidenced by the formation of a single peak at around  $\delta = 9.0$ . Solvent from the reaction mixture was then concentrated to a quarter of its original volume under reduced pressure. To this was added anhydrous  $\text{Et}_2\text{O}$  (30 mL), and stirred for another 10 minutes to obtain an orange yellow crystalline precipitate, which was filtered, washed with diethyl ether and dried under vacuum. The filtrate on cooling also gave a second crop. The combined yield of the products tend to be in the 90–98% range.

**Typical procedure for the enantioselective hydrogenation:** Catalyst **2b** (1.1 mg, 0.0007 mmol, 0.2 mol%), *trans*-1,2-diphenylpropene (60 mg, 0.31 mmol) and  $\text{CH}_2\text{Cl}_2$  (120 mL) were added to a vial with a stir bar. The vial was capped with a septum equipped with a needle outlet and put into a hydrogen autoclave. The autoclave was sealed and pressurized to 50 bar with  $\text{H}_2$ , and the mixture with stirred for 2 h. The solution was passed through a short silica gel plug (20%  $\text{EtOAc}$ /hexanes), then the eluent was analyzed by GC (100 °C; retention time,  $t_1 = 115.3$  min,  $t_2 = 118.5$  min using a chiral column prepared by Vigh et al.<sup>[34]</sup> (30.7 m  $\times$  0.25 mm, 30%  $\beta$ -*tert*-butyldimethylsilyl cyclodextrin derivative in OV-1701-vi of 0.25  $\mu\text{m}$  film thickness). Control experiments confirmed that reactions performed in parallel and on the small scale described above give the same results as ones on a larger scale occupying the whole autoclave. Absolute configuration of the product in Table 1 was determined by comparison of optical rotations with those reported by Buchwald.<sup>[6]</sup> The absolute configurations of the product shown in Table 2 was not determined but was tentatively assigned by analogy with the data presented in Table 1. The absolute stereochemistries of the products in Reactions (2) and (3) were not determined. The absolute configuration of the 2-phenylpropane formed in Reaction (6) was determined by comparison of optical rotations with those reported by Paquette et al.<sup>[35]</sup> and the absolute configurations of the other products in Reactions (4)–(6) were assumed by analogy with that work.

## Acknowledgements

We thank Ms. Xiuhua Cui and Dr. Mark T. Powell for preparation of intermediates in the syntheses of ligands **2g** and **2h**, Benjamin S. Lane for help with the GC/MS measurements, and Dr. Bob Taylor at A&M for help with deuterium NMR experiments. We also thank Dr. Richard Teichman at Johnson Matthey for valuable discussions. Support for this work was provided by Johnson Matthey and by The Robert A. Welch Foundation.

[1] R. K. Halterman, K. P. C. Vollhardt, M. E. Welker, *J. Am. Chem. Soc.* **1987**, *109*, 8105–8107.

- [2] R. L. Halterman, K. P. C. Vollhardt, *Organometallics* **1988**, *7*, 883–892.
- [3] F. R. W. P. Wild, J. Zsolnai, G. Huttner, H. H. Brintzinger, *J. Organomet. Chem.* **1982**, *232*, 233–247.
- [4] R. Waymouth, P. Pino, *J. Am. Chem. Soc.* **1990**, *112*, 4911–4914.
- [5] R. B. Grossman, R. A. Doyle, S. L. Buchwald, *Organometallics* **1991**, *10*, 1501–1505.
- [6] R. D. Broene, S. L. Buchwald, *J. Am. Chem. Soc.* **1993**, *115*, 12569–12570.
- [7] M. V. Troutman, D. H. Appella, S. L. Buchwald, *J. Am. Chem. Soc.* **1999**, *121*, 4916–4917.
- [8] R. H. Crabtree, G. E. Morris, *J. Organomet. Chem.* **1977**, *135*, 395–403.
- [9] R. Crabtree, *Acc. Chem. Res.* **1979**, *12*, 331–337.
- [10] R. H. Crabtree, R. J. Uriarte, *Inorg. Chem.* **1983**, *22*, 4152–4154.
- [11] R. H. Crabtree, P. C. Demou, D. Eden, J. M. Mihelcic, C. A. Parnell, J. M. Quirk, G. E. Morris, *J. Am. Chem. Soc.* **1982**, *104*, 6994–7001.
- [12] A. Lightfoot, P. Schnider, A. Pfaltz, *Angew. Chem.* **1998**, *110*, 3047–3050; *Angew. Chem. Int. Ed.* **1998**, *37*, 2897–2899.
- [13] D. G. Blackmond, A. Lightfoot, A. Pfaltz, T. Rosner, P. Schnider, N. Zimmermann, *Chirality* **2000**, *12*, 442–449.
- [14] G. Helmchen, A. Pfaltz, *Acc. Chem. Res.* **2000**, *33*, 336–345.
- [15] D.-R. Hou, K. Burgess, *Org. Lett.* **1999**, *1*, 1745–1747.
- [16] D.-R. Hou, J. Reibenspies, K. Burgess, *J. Org. Chem.* **2001**, *66*, 206–215.
- [17] J. K. Whitesell, *Chem. Rev.* **1989**, *89*, 1581–1590.
- [18] N. Hishida, N. Takada, M. Yoshimura, T. Sonoda, H. Kobayashi, *Bull. Chem. Soc. Jpn.* **1984**, *57*, 2600–2604.
- [19] M. Brookhart, B. Grant, A. F. Volpe, *Organometallics* **1992**, *11*, 3920–3922.
- [20] R. H. Crabtree, M. W. Davis, *J. Org. Chem.* **1986**, *51*, 2655–2661.
- [21] R. Kuwano, K. Sato, T. Kurokawa, D. Karube, Y. Ito, *J. Am. Chem. Soc.* **2000**, *122*, 7614–7615.
- [22] W. Chen, L. Xu, C. Chatterton, J. Xiao, *Chem. Commun.* **1999**, 1247–1248.
- [23] J. H. Davis Jr., K. J. Forrester, *Tetrahedron Lett.* **1999**, *40*, 1621–1622.
- [24] C. W. Lee, *Tetrahedron Lett.* **1999**, *40*, 2461–2464.
- [25] L. Green, I. Hemeon, R. D. Singer, *Tetrahedron Lett.* **2000**, *41*, 1343–1346.
- [26] L. Xu, W. Chen, J. Xiao, *Organometallics* **2000**, *19*, 1123–1127.
- [27] C. E. Song, E. J. Roh, *Chem. Commun.* **2000**, 837–838.
- [28] R. Hilgraf, A. Pfaltz, *Synlett* **1999**, 1814–1816.
- [29] Y. Sun, C. LeBlond, J. Wang, D. G. Blackmond, *J. Am. Chem. Soc.* **1995**, *117*, 12647–12648.
- [30] Y. Sun, J. Wang, C. LeBlond, R. A. Reamer, J. Laquidara, J. R. Sowa-Jr., D. G. Blackmond, *J. Organomet. Chem.* **1997**, *548*, 65–72.
- [31] J. M. Brown, A. E. Derome, G. D. Hughes, P. K. Monaghan, *Aust. J. Chem.* **1992**, *45*, 143–153.
- [32] H. Rottendorf, S. Sternhell, J. R. Wilmschurst, *Aust. J. Chem.* **1965**, *18*, 1759–1773.
- [33] A. P. Uijtewaal, F. L. Jonkers, A. v. d. Gen, *J. Org. Chem.* **1978**, *43*, 3306–3311.
- [34] A. Shitangkoon, G. Vigh, *J. Chromatography A* **1996**, *738*, 31–42.
- [35] L. A. Paquette, M. R. Sivik, E. I. Bzowej, K. J. Stanton, *Organometallics* **1995**, *14*, 4865–4878.
- [36] Crystallographic data (excluding structure factors) for the structures reported in this paper have been deposited with the Cambridge Crystallographic Data Centre as supplementary publication no. CCDC-166174 (**2j**), -166175 (**2b**), -166176 (**2i**), and -166177 (**2h**). Copies of the data can be obtained free of charge on application to CCDC, 12 Union Road, Cambridge CB21EZ, UK (fax: (+44) 1223-336-033; e-mail: deposit@ccdc.cam.ac.uk).

Received: May 2, 2001 [F3229]